Journal of Applied Polymer Science

Effect of the maleation of lignosulfonate on the mechanical and thermal properties of lignosulfonate/poly(ε-caprolactone) blends

Fei Wang,[1,2] Xuping Yang,[1,2] Yangxue Zou[1,2]

[1]School of Materials Science and Engineering, Southwest University of Science and Technology, Mianyang, Sichuan 621010, China

[2]Engineering Research Center for Biomass Materials (Ministry of Education), Mianyang, Sichuan 621010, China

Correspondence to: X. Yang (E-mail: yangxupingyxp@163.com)

ABSTRACT: Maleated lignosulfonate (MLS) produced by esterification with maleic anhydride and unmodified lignosulfonate [in the form of lignosulfonic acid (LS)] were incorporated into poly(ε-caprolactone) (PCL) via melt-blending. The obtained MLS/PCL composites and LS/PCL composites were characterized by Fourier transform infrared (FTIR) spectroscopy, differential scanning calorimetry (DSC), thermogravimetric (TG) analysis, and electronic universal testing. The FTIR and DSC results show that the interactions between MLS and PCL were stronger than those between LS and PCL, whereas the TG analysis indicated that the LS/PCL composite was more thermally stable than the MLS/PCL composite. The tensile strength of the MLS/PCL blends remained at about 18 MPa when the MLS content reached 50 wt %; this was about 1.7 times larger than that of the LS/PCL blend. The Young's modulus was also enhanced; this indicated an improvement in the mechanical properties. The results show that the maleation of lignosulfonate was beneficial for enhancing the mechanical properties of these blends. © 2015 Wiley Periodicals, Inc. J. Appl. Polym. Sci. **2016**, *133*, 42925.

KEYWORDS: maleated lignosulfonate; mechanical property; melt blending; poly(ε-caprolcatone); thermal property

Received 11 June 2015; accepted 7 September 2015

DOI: 10.1002/app.42925

INTRODUCTION

With the depletion of fossil fuel resources and growing concerns about the environment, more and more efforts have gone into renewable and biodegradable polymers. Lignocellulosic materials containing cellulose, hemicelluloses, and lignin are of great interest. Lignin, which is the most abundant aromatic polymer in nature[1,2] and is largely present in the cell walls of vascular plants and woody tissues, together with cellulose and hemicelluloses, has attracted much attention recently because of its biodegradability, renewability, and nontoxic. Generally, lignin is cogenerated in the pulp and papermaking industries and biofuel production processes; more than 70 million tons are produced just from papermaking.[3] However, only a small amount (1–2%) of the lignin generated form papermaking is used in a wide range of specialty products,[1] whereas the rest is burned for energy generation in the same mills.

The productive utilization of lignin has been sought for decades, and thermoplastics based on lignin have been considered as one especially attractive method.[4] Many synthetic polymers have been incorporated with lignin[5–8]; these include poly(ethylene oxide), polypropylene (PP), poly(vinyl chloride) (PVC), and poly(ethylene terephthalate). However, lignin, a polar material, has poor compatibility with nonpolar synthetic polymers, such as polyethylene and PP, and this results in the deterioration of the mechanical properties of various polymers in blends. The tensile and impact properties of PVC–lignin blends deteriorated in comparison with those of pure PVC when the blends were produced through melt compounding,[7] although PVC and lignin were miscible when they were blended in solution.[9] Poly (butyrate succinate)–lignosulfonate blends[10] and poly(L-lactic acid) and lignin blends[11] also suffered deterioration in some mechanical properties, despite the interactions found between lignin and the carbonyl groups of polyesters. To obtain much better compatibility between lignin and other polymers, the esterification and graft copolymerization of lignin[12–16] and the addition of compatibilizers[17] are often used. Partly acetylated softwood kraft lignin has compatibility with low-density polyethylene, PP, polystyrene, and poly(ethylene terephthalate) according to the literature, and the tensile strength and breaking strain of these blends almost did not change with modified lignin contents up to 12.5 wt %.[13]

Poly(ε-caprolactone) is a long-chain polyester that is hydrophobic and semicrystalline and the chemical structure of which leads to its flexibility and biodegradability. The carbonyl groups in poly(ε-caprolactone) (PCL) molecules contribute to hydrogen-bond formation with the hydroxyl groups of lignin.

Table I. Compositions of the Samples and Thermal Properties from DSC and TG

Sample	PCL in the blend (wt %)	MLS in the blend (wt %)	LS in the blend (wt %)	ΔH_m (J/g)	ΔH_c (J/g)	χ_c (%)[a]	T_0 (°C)	Char residue at 750°C (%)
MLS/PCL-0	100	0	0	65.60	59.89	48.2	381	0.60
MLS/PCL-10	90	10	0	65.21	52.62	47.9	327	5.53
MLS/PCL-20	80	20	0	57.34	47.51	42.2	243	9.32
MLS/PCL-30	70	30	0	53.00	42.19	39.0	234	13.35
MLS/PCL-40	60	40	0	45.40	38.42	33.3	222	16.22
MLS/PCL-50	50	50	0	37.88	29.65	27.8	223	22.16
MLS/PCL-100	0	100	0	ND	ND	ND	184	37.80
LS/PCL-10	90	0	10	62.00	55.29	45.6	385	5.04
LS/PCL-20	80	0	20	54.60	50.98	40.1	333	9.86
LS/PCL-30	70	0	30	49.07	45.07	36.1	296	14.94
LS/PCL-40	60	0	40	44.23	39.79	32.5	262	21.89
LS/PCL-50	50	0	50	35.12	31.65	25.8	257	24.25
LS/PCL-100	0	0	100	ND	ND	ND	182	51.24

ND, not detected.
[a] $\chi_c = \Delta H_m/\Delta H_{m,\infty}$, where $\Delta H_{m,\infty}$ (136 J/g) is the enthalpy of fusion of 100% crystalline PCL and ΔH_m is the enthalpy of fusion of different polymer composite.[28]

Therefore, it is reasonable to blend PCL with lignin to prepare composites with better properties. However, according to Puciariello *et al.*,[18] straw lignin–PCL blends prepared by high-energy ball milling were immiscible. Teramoto *et al.*,[15] to improve the compatibility between lignin and PCL, modified organosolv lignin with acyl anhydrides and then blended it with PCL by solution mixing and found that the blends of organosolv lignin esters (carbon numbers 3–5) were miscible on a glass-transition-temperature detection scale.

The blending PCL with lignin and the blends prepared in melt blending, which are easily scaled up, can greatly reduce their cost. However, according to Li *et al.*,[19] PCL–lignin blends prepared through mechanical mixing did not show any miscibility compared with blends prepared via solution casting, which did show miscibility. Therefore, in this study, lignosulfonate was modified with maleic anhydride, which provided carboxyl groups and double bonds, and was then blended with PCL via melt blending to obtain composites with enhanced properties. In the meantime, unmodified lignosulfonate in the form of lignosulfonic acid (LS) was also incorporated into the PCL matrix in the same way as a comparison. The thermal stability and mechanical properties were determined by differential scanning calorimetry (DSC), thermogravimetric (TG) analysis, and electronic universal testing in this study.

EXPERIMENTAL

Materials

Commercial-grade poly(ε-caprolactone) (800C), with a number-average molecular weight of 80,000 g/mol (polydispersity index = 1.8), was used as received. It was obtained from Brightchina Bio-Engineering High-Tech Enterprises. All of the reagents listed next were purchased from Chengdu Kelong Chemical Reagent Factory. The sodium lignosulfonate used in this study was a laboratory reagent, with water-insoluble matter of less than 4 wt %. Maleic anhydride [analytical reagent (AR), ≥99.5%] and sodium hydroxide (AR, ≥96%) were used without further purification. Sulfuric acid (AR, 95.0–98.0 wt %) was diluted to 1.8 mol/L with distilled water before use.

Preparation of Esterified Lignosulfonate

Esterified lignosulfonate or maleated lignosulfonate (MLS) was synthesized in alkaline aqueous under mild heating conditions. The specific reaction conditions were consistent with what we have reported before.[20] LS was obtained from sodium lignosulfonate, which was acidized in a water solution. The structural properties of MLS were characterized by Fourier transform infrared (FTIR) spectroscopy.

Synthesis of the Blends of Esterified Lignosulfonate and PCL

The blends were prepared through melt-blending in a Haake torque rheometer incorporating a mixer (Rheomix 600 OS) at different MLS/PCL weight ratios from 0:100 up to 50:50, as shown in Table I. The two components were manually mixed with different weight ratios before they were added to the mixer. The blending temperature was 120°C, and the rotation speed of rotors was 60 rpm. The blending lasted for 10 min for every sample. Then, the blending samples were cut into small pieces with a knife and molded into dumbbell shapes and strip specimens at 120°C and 120 MPa. The LS/PCL blends were prepared under the same conditions.

FTIR Analysis

LS and MLS were characterized with an FTIR spectrometer (Nicolet 6700) to determine changes in the functional groups, especially carbonyl groups. Each sample was ground into powder and then pressed into pellet form with KBr at a weight ratio of 1:60. The pellets were scanned 32 times from 4000 to 400 cm^{-1} with a spectral resolution of 4 cm^{-1}.

The blending samples could not be ground into powder and were lightproof. As a result, the structural changes after

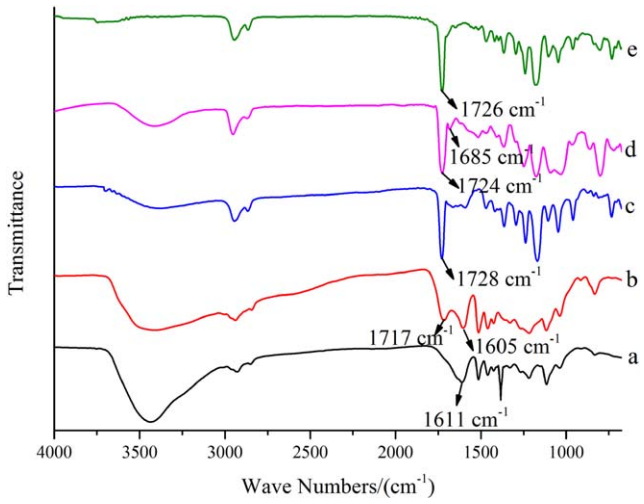

Figure 1. FTIR spectra of (a) LS, (b) MLS, (c) PCL, (d) PCL/MLS blends (containing 10 wt % MLS), and (e) LS/PCL blends (containing 10 wt % LS). [Color figure can be viewed in the online issue, which is available at wileyonlinelibrary.com.]

blending of the samples were determined in attenuated total reflectance mode with a resolution of 4 cm^{-1}. Each sample was scanned 32 times from 4000 to 670 cm^{-1}.

DSC Analysis

The DSC experiments were carried out on a TA Instruments Q200 instrument to determine the thermal properties of the samples. The samples, which weighed 5–6 mg, were scanned from ambient temperature to 120°C in aluminum pans at a heating rate of 10°C/min and were then cooled to −10°C at the same cooling rate under a flowing nitrogen atmosphere (50 mL/min) to eliminate their thermal histories. Then, the samples were heated to 200°C under the same heat conditions.

TG Analysis

The thermal stability and decomposition of the samples were studied by TG analysis (TA Instrument Q200) with platinum pans with about 5 mg samples in each case. The samples were heated under a nitrogen atmosphere with a flow rate of 20 mL/min from ambient temperature to 750°C, and the heating rate was 20°C/min.

Mechanical Properties

The tensile properties of the blending samples were characterized with an electronic universal testing machine (MTS Criterion model 45) according to ISO 527-2, specifically with type 1BA with a gauge length of 25 mm. The tensile speed was 20 mm/min. The notched impact properties were tested with a Charpy impact tester (ZBC 7000) according to ISO 179-1. At least five specimens were tested for each composite.

RESULTS AND DISCUSSION

FTIR Analysis

The chemical structure of MLS was obviously different from that of LS, as shown in Figure 1. The appearance of a peak of MLS centered at 1717 cm^{-1} [Figure 1(b)], compared with that of LS [Figure 1(a)], was evidence for successful maleation, and other peaks and their assignments were reported in our previous work.[20]

FTIR spectroscopy is a quite suitable technique for investigating the crystallinity and the existence of specific interactions of polymer blend systems. The spectra of the pure PCL (spectrum c), MLS/PCL composite at a weight ratio of 10:90 (spectrum d), and LS/PCL composite at a weight ratio of 10:90 (spectrum e) are depicted in Figure 1. In the spectrum of the pure PCL, a weak sorption band centered at 3375 cm^{-1} was assigned to the stretching of low-concentration hydroxyl chain-end groups of PCL.[19,21] The absorptions of asymmetric and symmetric C—H stretching vibrations were located at 2944 and 2866 cm^{-1}, respectively, and the weak bands at 1469 and 1416 cm^{-1} were also ascribed to C—H vibrations, bending for the former and scissoring for the latter.[22] The peak centered at 1728 cm^{-1} of PCL was ascribed to C═O stretching vibrations, which could be divided into two peaks in its second derivative curve (not shown). One peak was associated with the amorphous fraction situated at 1737 cm^{-1}, and a shoulder at 1720 cm^{-1} corresponded to the C═O stretching in the crystalline part of PCL; this was consistent with the reported literature.[19] Major peaks in the spectrum centered in the range from 1300 to 1000 cm^{-1} were attributed to C—O—C and C—O vibrations.[21,23]

After melt blending, the C═O absorption band of the PCL blended with MLS shifted to a lower frequency (from 1728 to 1724 cm^{-1}), and a weak band at 1685 cm^{-1}, which was attributed to C═O absorption of MLS, also shifted to a lower frequency from 1717 cm^{-1}, as shown in Figure 2. The wavenumber shifts of the C═O absorption of PCL in blends

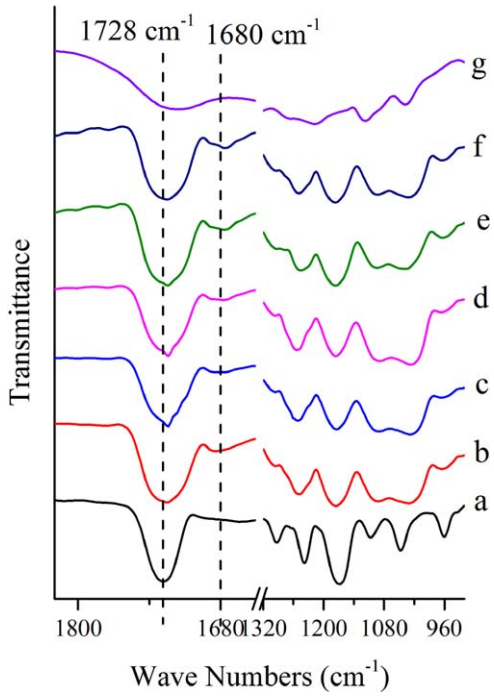

Figure 2. FTIR spectra in the regions (A) 1790–1680 and (B) 1320–930 cm^{-1} for the (a) pure PCL; MLS/PCL blends with MLS contents of (b) 10, (c) 20, (d) 30, (e) 40, and (f) 50 wt %; and (g) MLS. [Color figure can be viewed in the online issue, which is available at wileyonlinelibrary.com.]

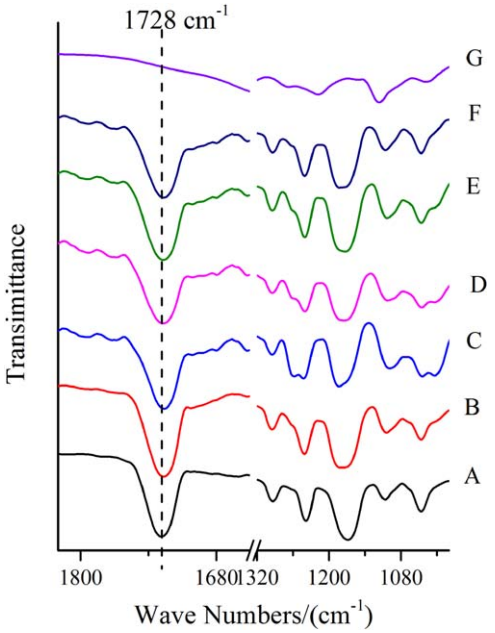

Figure 3. FTIR spectra in the regions (A) 1790–1680 and (B) 1320–930 cm^{-1} for the (A) pure PCL; LS/PCL bends with LS contents of (B) 10, (C) 20, (D) 30, (E) 40, and (F) 50 wt %; and (G) LS. [Color figure can be viewed in the online issue, which is available at wileyonlinelibrary.com.]

containing different proportions of MLS were almost invariant,[8] whereas the wave-number shifts of C═O of MLS in the blends shifted to lower wave numbers (from 1685 to 1676 cm^{-1}) with an increase in MLS. Compared with the MLS/PCL composites, the LS/PCL composites (shown in Figure 3) also showed a peak shift of C═O from 1728 to 1726 cm^{-1}, but there was no peak between 1700 and 1660 cm^{-1} because of the inexistence of C═O on the LS molecules. The changes in the peak locations and intensities evidenced interactions, such as hydrogen bonds, existing between PCL and MLS and PCL and LS.[24] The intensity of the peak centered around 1100 cm^{-1} of the PCL blended with MLS, which was assigned to ═C—O—C vibrations,[23] was much stronger than that of the pure PCL and PCL blended

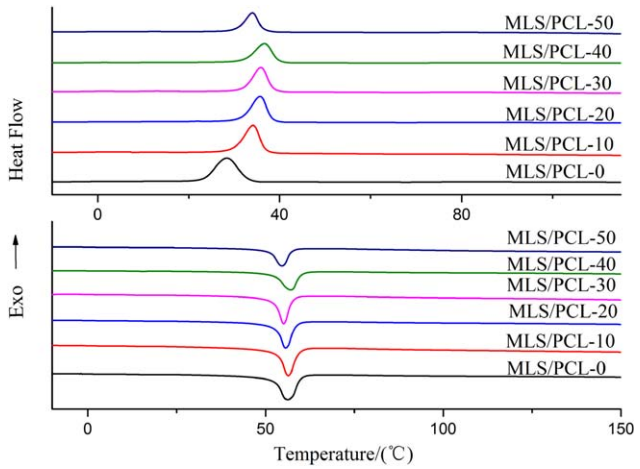

Figure 4. DSC curves of the PCL and MLS/PCL blends. [Color figure can be viewed in the online issue, which is available at wileyonlinelibrary.com.]

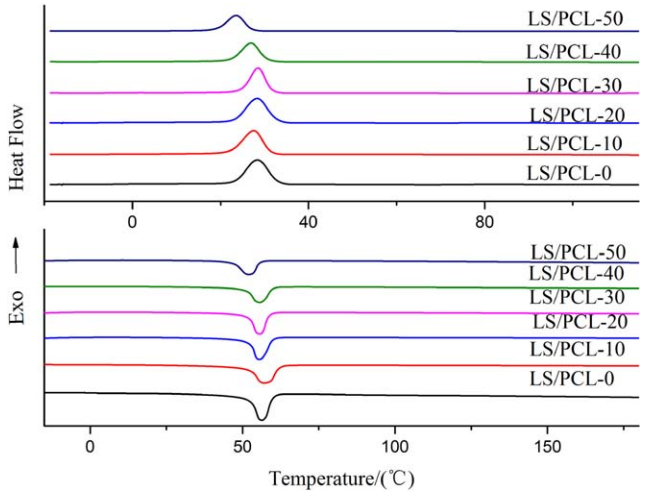

Figure 5. DSC curves of the PCL and LS/PCL blends. [Color figure can be viewed in the online issue, which is available at wileyonlinelibrary.com.]

with LS, as shown in Figures 2 and 3; this probably resulted from the further esterification of carboxyl groups induced via maleation with alcohol hydroxyl groups.[24] Therefore, the maleation of lignosulfonate contributed to better interactions between the components PCL and lignosulfonate.

DSC Analysis

DSC is usually used to obtain thermal behavior information, such as the crystallization temperature (T_c) and melting temperature (T_m), and to some extent, changes that can be used to indirectly show interactions between the components in polymer blends.[19–25] In this study, T_c and T_m were obtained to evaluate the thermal properties of the lignin on PCL in the blend.

The DSC thermograms of the pure PCL, MLS/PCL composites with different weight ratios of MLS, and LS/PCL composites with different weight ratios of LS are shown in Figures 4 and 5, respectively. With increasing MLS content, the MLS/PCL composites showed a slight depression in T_m and T_c values that were much higher than those of the pure PCL; this indicated interactions between MLS and PCL.[26,27] The T_m values of the LS/PCL composites also showed a depression with the addition of LS; this also indicated interactions between LS and PCL, whereas the T_c values were equal to or slightly higher than those of pure PCL when the LS content was below 30 wt % and were lower than those of pure PCL when the LS content reached 40 wt % because of the aggregation of LS phases in the PCL matrices.[10] The lower degree of supercooling (ΔT) of the MLS/PCL composites, which indicated a significant equilibrium melting point depression, was evidence of stronger interactions between MLS and PCL than those between LS and PCL.[27] The stronger interactions between MLS and PCL resulted in a finer dispersion of MLS in PCL; this was attributed to the carboxyl groups and double bonds induced via maleation reactions, which could provide sites for hydrogen bonding and even further esterification under high temperatures and shear rates; this was consistent with the FTIR results. Both the addition of MLS and LS led to lower crystallization degrees (χ_cs), as shown in Table I; this resulted because the interactions between the components

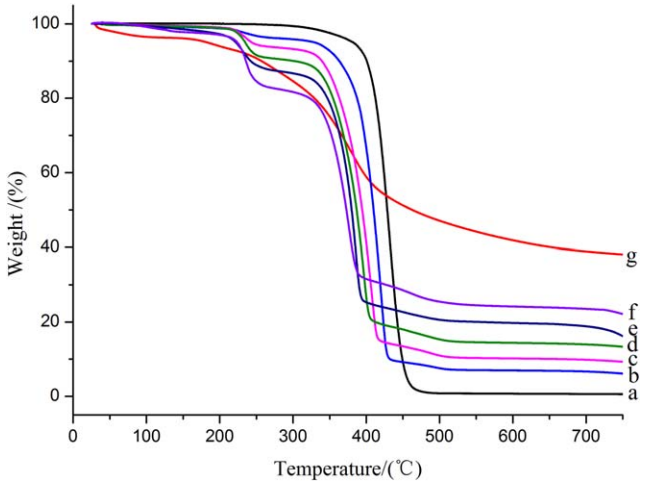

Figure 6. TG curves of the (a) pure PCL, (b) MLS/PCL-10, (c) MLS/PCL-20, (d) MLS/PCL-30, (e) MLS/PCL-40, (f) MLS/PCL-50, and (g) MLS. [Color figure can be viewed in the online issue, which is available at wileyonlinelibrary.com.]

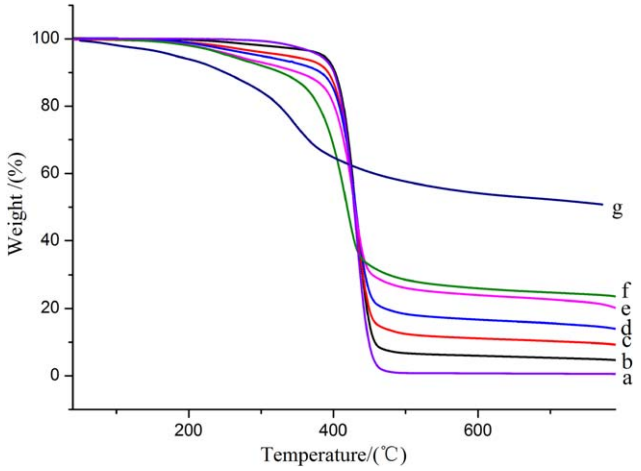

Figure 7. TG curves of the (a) pure PCL, (b) LS/PCL-10, (c) LS/PCL-20, (d) LS/PCL-30, (e) LS/PCL-40, (f) LS/PCL-50, and (g) LS. [Color figure can be viewed in the online issue, which is available at wileyonlinelibrary.com.]

restrained the mobility of the PCL molecules. The higher χ_c of the MLS/PCL composites may have been due to the higher T_c and enthalpy of crystallization (ΔH_c) and lower ΔT compared to those of the LS/PCL composites.[27,29]

TG Analysis

TG analysis is a suitable method for studying the thermal stability and decomposition processes of polymers and polymer blends. The TG curves of the pure PCL, MLS/PCL blends, and LS/PCL blends are shown in Figures 6 and 7. PCL was thermally stable up to 300°C and decomposed in one step in the temperature range 380–480°C. The char residue of PCL was lower than 1% when the temperature reached 500°C. The TG curves of the MLS/PCL blends showed multistep decomposition processes under a nitrogen atmosphere, as shown in Figure 6. The weight loss was due to the evaporation of free and bonded water and occurred below 150°C.[30] The onset temperature (T_0) of thermal decomposition, which was the temperature at a weight loss of 5 wt %, decreased from 381°C (of the pure PCL) to 234°C (of the MLS/PCL blend with a MLS weight ratio of 50%), and the char residues of the MLS/PCL blends increased with increasing MLS addition because of the addition of MLS, as shown in Table I. The temperature of the maximum decomposition rate (T_{max}) of the MLS/PCL blends decreased linearly with increasing MLS content, as shown in Figure 8; this indicated that MLS and PCL were partially compatible.[31]

Compared with the MLS/PCL blends, the LS/PCL blends presented a different variation trend of T_{max} as a function of the LS content, as shown in Figure 8; T_{max} remained at about 432°C up to 30 wt % addition of LS. T_{max} was 417.68°C when the LS content reached 50 wt %; this was much higher than that of LS. The T_0s of the MLS/PCL blends also decreased with increasing LS contents, but they were higher than those of LS/PCL; this was probably due to the maleation of LS. The char residues of the LS/PCL blends were also higher than that of MLS/PCL; this was consistent with the relationship between LS's char residue and MLS's char residue. Therefore, the LS/PCL blends were more thermally stable than the MLS/PCL blends, whereas the interactions between LS and PCL may have been weaker than those between MLS and PCL because the thermal degradation process of the LS/PCL blends did not changed as much as that of the MLS/PCL blends.

Mechanical Properties

The mechanical properties of polymer blends are of great importance for their practical applications and depend highly on the miscibility or compatibility between components.

The tensile properties of the pure PCL and MLS/PCL and LS/PCL composites were characterized via the tensile strength, elongation at break, and Young's modulus, as shown in Table II. PCL is a ductile polymer with an elongation at break of 994.7%; it undergoes great deformation when tensioned. However, the relatively lower modulus (195.5 MPa) renders its

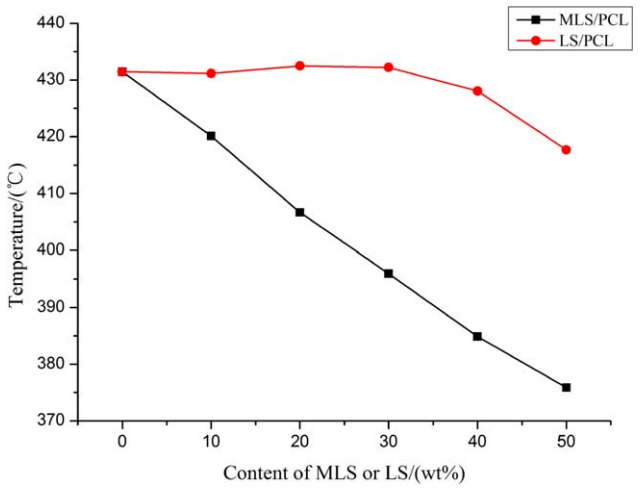

Figure 8. T_{max} values of the MLS/PCL blends and LS/PCL blends as a function of the MLS or LS content. [Color figure can be viewed in the online issue, which is available at wileyonlinelibrary.com.]

Table II. Mechanical Properties of the Samples

Sample	Tensile strength (MPa)	Elongation at break (%)	Young's modulus (MPa)	Impact strength (kJ/m^2)
MLS/PCL-0	23.02 ± 1.6	994.7 ± 15.1	195.5 ± 7.9	6.01 ± 0.28
MLS/PCL-10	20.35 ± 1.2	836.1 ± 13.4	271.1 ± 12.0	3.98 ± 0.15
MLS/PCL-20	19.65 ± 1.2	612.9 ± 11.0	413.4 ± 11.7	2.98 ± 0.17
MLS/PCL-30	18.96 ± 0.9	268.5 ± 6.2	535.3 ± 12.5	2.16 ± 0.17
MLS/PCL-40	18.42 ± 0.6	97.2 ± 3.5	612.2 ± 12.3	1.79 ± 0.10
MLS/PCL-50	17.91 ± 0.3	37.0 ± 1.8	736.9 ± 14.3	1.67 ± 0.11
LS/PCL-10	21.11 ± 1.4	800.3 ± 11.9	277.0 ± 11.3	3.66 ± 0.16
LS/PCL-20	16.58 ± 0.5	436.7 ± 6.3	362.1 ± 10.7	2.63 ± 0.16
LS/PCL-30	14.72 ± 0.6	110.9 ± 3.3	410.8 ± 12.8	1.98 ± 0.14
LS/PCL-40	13.47 ± 0.3	35.4 ± 1.5	500.5 ± 12.9	1.56 ± 0.11
LS/PCL-50	10.60 ± 0.4	10.2 ± 0.4	645.1 ± 12.3	1.40 ± 0.10

practical applications in many cases where a strong rigidity is needed.[19] The Young's modulus of PCL increased significantly when it was blended with LS, especially when the content of LS reached 50 wt %; the Young's modulus of the LS/PCL composite (645 MPa) was three times larger than that of the pure PCL. However, the other tensile properties of the LS/PCL blends decreased to varying degrees; this was consistent with the literature[10,19] and was due to the poor adhesion between the LS particles and PCL phases. In contrast, the tensile strength of the MLS/PCL composites was much higher (1.7-fold) than that of the LS/PCL composites when the content reached 50%; this was ascribed to the stronger adhesion between MLS particles and PCL phases and the finer dispersion of MLS in the PCL matrix. The Young's modulus of the MLS/PCL blends was also higher than that of the LS/PCL blends; this was due to the higher χ_c of the MLS/PCL blends. The increasing rate of Young's modulus of MLS/PCL was a little bigger than that of the LS/PCL blends; this indicated different interactions and distributions. The elongation at break of MLS/PCL also decreased drastically, as the rigid particles could not deform. The impact strength data of the pure PCL and MLS/PCL and LS/PCL composites were also determined, as shown in Table II. The addition of MLS and LS, both of which were brittle materials, resulted in a lower impact strength in the composites.[17] The slight increase in the impact strength of the MLS/PCL composites may have been due to the finer dispersion of MLS, as discussed previously.

CONCLUSIONS

Lignosulfonate esterified with maleic anhydride (MLS) and LS were incorporated into PCL separately via melt-blending with a weight ratio of up to 50%. The intensified peak centered at 1100 cm^{-1} and the larger frequency shift of C=O compared with the LS/PCL blends evidenced stronger interactions between MLS and PCL than those between LS and PCL, as shown in FTIR–attenuated total reflectance. The depression in T_m and decrease in ΔT also gave indirect evidence for interactions between the two components. The mechanical properties of the composites were improved by the maleation of lignosulfonate. Particularly, the tensile strengths of the MLS/PCL blends remained at about 18 MPa when the MLS content reached 50 wt %; this was about 1.7 times larger than that of the LS/PCL blend. Although the maleation of lignosulfonate contributed to the compatibility, the thermal stability of the MLS/PCL composites was worse than that of the LS/PCL composites. The maleation of lignosulfonate in the alkaline water solution provided an inexpensive and easy method for the compatibilization of lignosulfonate and PCL. This contributed to the utilization of lignosulfonate; this is a byproduct of the papermaking industry. MLS/PCL composites with dark color could be used as biodegradable materials for agricultural ground films and could contribute to improvements in the soil temperature, keeping soil warm and watered, and preventing soil compaction.

ACKNOWLEDGMENTS

This work was financially supported by the State Natural Science Funds Commission/Chinese Academy of Engineering Physics (contract 11176025) and the Open Project of State Key Laboratory Cultivation Base for Nonmetal Composites and Functional Materials of the Southwest University of Science and Technology key research platform professional scientific research team building innovation fund projects (Mianyang, China, contract grant number 14tdsc02).

REFERENCES

1. Lora, J. H.; Glasser, W. G. *J. Polym. Environ.* **2002**, *10*, 39.
2. Chen, C. Z.; Li, M. F.; Wu, Y. Y.; Sun, R. C. *RSC Adv.* **2014**, *4*, 16944.
3. Kumar, M. N. S.; Mohanty, A. K.; Erickson, L.; Misra, M. *J. Biobased Mater. Bioenergy* **2009**, *3*, 1.
4. Saito, T.; Brown, R. H.; Hunt, M. A.; Pickel, D. L.; Pickel, J. M.; Messman, J. M.; Baker, F. S.; Keller, M.; Naskar, A. K. *Green Chem.* **2012**, *14*, 3295.
5. Kubo, S.; Kadla, J. F. *J. Appl. Polym. Sci.* **2005**, *98*, 1437.
6. Alexy, P.; Kosikova, B.; Podstranska, G. *Polymer* **2000**, *41*, 4901.

7. Yue, X. P.; Chen, F. G.; Zhou, X. S.; He, G. J. *Int. J. Polym. Mater.* **2012**, *61*, 214.
8. Mousavioun, P.; Doherty, W. O. S.; George, G. *Ind. Crops Prod.* **2010**, *67*, 3151.
9. Mishra, S. B.; Mishra, A. K.; Kaushik, N. K.; Khan, M. A. *J. Mater. Process. Technol.* **2007**, *183*, 273.
10. Lin, N.; Fan, D. K.; Chang, P. R.; Yu, J. H.; Cheng, X. C.; Huang, J. *J. Appl. Polym. Sci.* **2011**, *121*, 1717.
11. Li, J.; He, Y.; Inoue, Y. *Polym. Int.* **2003**, *52*, 949.
12. Maldhure, A. V.; Ekhe, J. D.; Deenadayalan, E. *J. Appl. Polym. Sci.* **2012**, *125*, 1701.
13. Jeong, H.; Park, J.; Kim, S.; Lee, J.; Cho, J. W. *Fiber Polym.* **2012**, *13*, 1310.
14. Li, Y.; Sarkanen, S. *Macromolecules* **2002**, *35*, 9707.
15. Teramoto, Y.; Lee, S. H.; Endo, T. *Polym. J.* **2009**, *41*, 219.
16. Nemoto, T.; Konishi, G. I.; Tojo, Y.; An, Y. C.; Funaoka, M. *J. Appl. Polym. Sci.* **2012**, *123*, 2636.
17. Sahoo, S.; Misra, M.; Mohanty, A. K. *Compos. A* **2011**, *42*, 1710.
18. Pucciariello, R.; Bonini, C.; Auria, M. D.; Villani, V.; Giammarino, G.; Gorrasi, G. *J. Appl. Polym. Sci.* **2008**, *109*, 309.
19. Li, J.; He, Y.; Till, F.; Inoue, Y. *Polym. J.* **2001**, *33*, 336.
20. Wang, F.; Yang, X.; Zou, Y. *Int. J. Polym. Anal. Chem.* **2015**, *20*, 69.
21. Elzein, T.; Nasser-Eddine, M.; Delaite, C.; Bistac, S.; Dumas, P. *J. Colloid Interfaces Sci.* **2004**, *273*, 381.
22. Shen, Z.; Hu, J.; Wang, J.; Zhou, Y. *Int. J. Environ. Sci. Technol.* **2015**, *12*, 1235.
23. Aghdam, R. M.; Najarian, S.; Shakhesi, S.; Khanlari, S.; Shaabani, K.; Sharifi, S. *J. Appl. Polym. Sci.* **2012**, *124*, 123.
24. John, J.; Mani, R.; Bhattacharya, M. *J. Polym. Sci. Part A: Polym. Chem.* **2002**, *40*, 2003.
25. Liang, Z. J.; Li, B.; Ruan, J. Q. *Polym. Test.* **2015**, *42*, 185.
26. Chen, C. C.; Chueh, J. Y.; Tseng, H.; Huang, H. M.; Lee, S. Y. *Biomaterials* **2003**, *24*, 1167.
27. Zhou, B.; Li, J.; He, Y. *Macromol. Biosci.* **2003**, *3*, 684.
28. Jian, W.; Ken, C. M.; Yongli, M. *Polymer* **2002**, *43*, 1357.
29. Xu, X.; He, Z.; Lu, S.; Guo, D.; Yu, J. *Macromol. Res.* **2014**, *22*, 1084.
30. Hatakeyama, H.; Hatakeyama, T. In Biopolymers: Lignin, Proteins, Bioactive Nanocomposites; Abe, A., Dusek, K., Kobayashi, S., Eds.; Springer: Berlin, **2010**; Vol. *232*, p 1.
31. Xu, Y. Z.; Wang, C. P.; Stark, N. M.; Cai, Z. Y.; Chu, F. X. *Carbohydr. Polym.* **2012**, *88*, 422.